

PAPER REF: 19917

ROTATIONAL STIFFNESS OF TIMBER-TO-TIMBER CONNECTIONS WITH SELF-TAPPING AXIALLY LOADED SCREWS

Sebastian Egner^(*), Matthias Frese

Karlsruhe Institute of Technology (KIT) – Timber Structures and Building Construction, Karlsruhe, Germany

^(*)*Email:* sebastian.egner@kit.edu

ABSTRACT

Self-tapping axially loaded screws provide high load-carrying capacity and great stiffness. Due to these advantages, they were preferably applied to realise connections for tension members. While the translational stiffness of those connections can be estimated for engineering purposes sufficiently, knowledge about the rotational stiffness is still low. The investigations reported here show the influence of the inclination and the geometrical arrangement of the self-tapping screws on the rotational stiffness of connections for tension members. A test set-up was therefore developed. It enables that tensile forces and rotation are simultaneously effective and quantitatively independently of each other. The experimental results show that the inclination of the screws and the resulting compressive stress in the shear plane has a major influence on the rotational stiffness and that the stiffness of the screws themselves becomes less effective.

Keywords: rotational stiffness, K_{ax} , axially loaded screws, self-tapping screws.

INTRODUCTION

Modern engineered timber structures with large components and wide spans require fasteners with high load-carrying capacity. The high load-carrying capacity and great stiffness of self-tapping axially loaded screws led to a rapid acceptance for these applications. The calculation of the load-carrying capacity of such connections is state of the art. So far, the translational connection stiffness (K_T) can be estimated with empirical equations for the axial stiffness (K_{ax}) of screws. These equations complement those for the lateral stiffness (K_{ser}) of screws which are based on the provisions for bolts and nails using the nominal diameter [1].

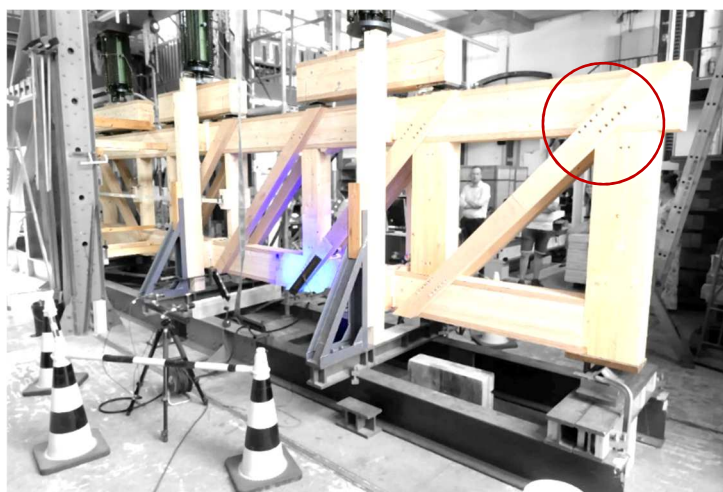


Fig. 1 – Truss girder with diagonals attached with inclined self-tapping axially loaded screws.

However, there are barely examinations on such connections how they mechanically perform under the common effect of tension and unintentional rotation. This effect is for instance known from non-hinged connections in truss girders as encircled in Figure 1. Under load relative rotations between members occur. Depending on the rotational stiffness (K_r) of the connection, this causes secondary stresses in the members and uneven forces in the single screws.

In order to better understand the complex stress distribution in connections with axially loaded screws and simultaneous rotation, a new test apparatus was developed. Therewith it is possible to experimentally simulate tension stress and simultaneously rotation. Furthermore, the quantity of tension stress and that of rotation can be steered independently of each other so that realistic stress conditions in truss girder connections can be studied. Particular attention is given to the dependence of the screw stiffnesses K_{ax} and K_{ser} on the respective loading direction.

THEORETICAL CONSIDERATIONS

The rotational stiffness K_r of a connection with dowel-type fasteners can be determined by equation (1) based on the connection stiffness (K) and the polar moment of inertia [2]. K is usually assumed to be constant meaning that the effect of varying load-to-grain angles is not reflected [3]. According to Eurocode 5 only the diameter of the fastener and the density of the lumber are taken into account.

$$K_r = K * \left(\sum_{i=1}^n x_i^2 + \sum_{i=1}^n y_i^2 \right) \quad (1)$$

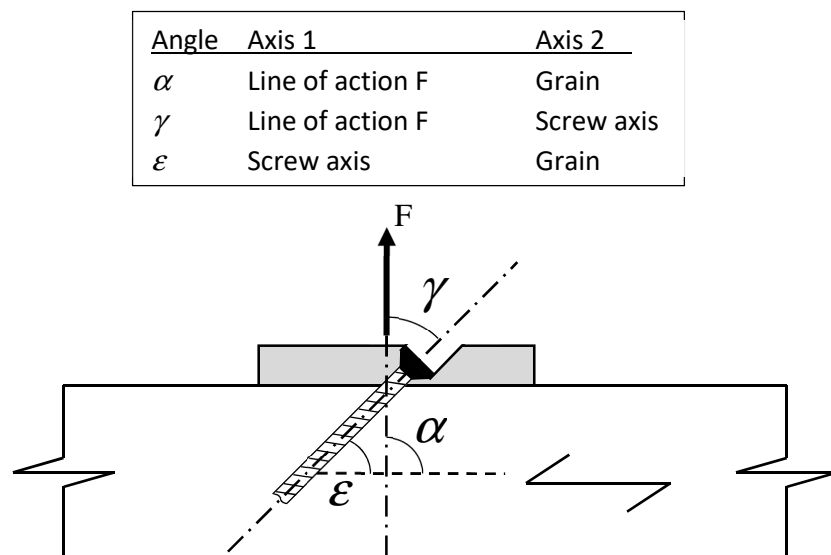


Fig. 2 – Angle relationships

However, the stiffness of axially loaded screws highly depends on a complex correlation between screw axis, grain and load direction [4]. The respective angle relationships are illustrated in Figure 2. It is therefore essential to consider the different stiffness behaviour that such screws exhibit in lateral and axial direction. There are different approaches available to calculate K_{ax} . Existing models take into account not only the diameter of the fastener and the density of the lumber but also the insertion length and the angle γ . More differentiated approaches also consider the angles α and ε . De Santis and Fragiaco [5] provide an overview

of different calculation approaches. In this study, the model equation (3) developed by Blaß and Steige [6] is used for the further calculations. Equation (3) is based on an angle $\gamma = 0^\circ$ and delivers the respective axial stiffness shares ($K_{ax,1}$ and $K_{ax,2}$) of the shear stiffness ($K_{s,ax}$) according to Equation (4). Figure 3, left illustrates the mechanical mode of action of both $K_{s,ax}$ and K_{ser} in a side member attached with an inclined screw. Figure 3 right exemplifies the relationship between six inclined screws and the connection stiffnesses K_r and K_t .

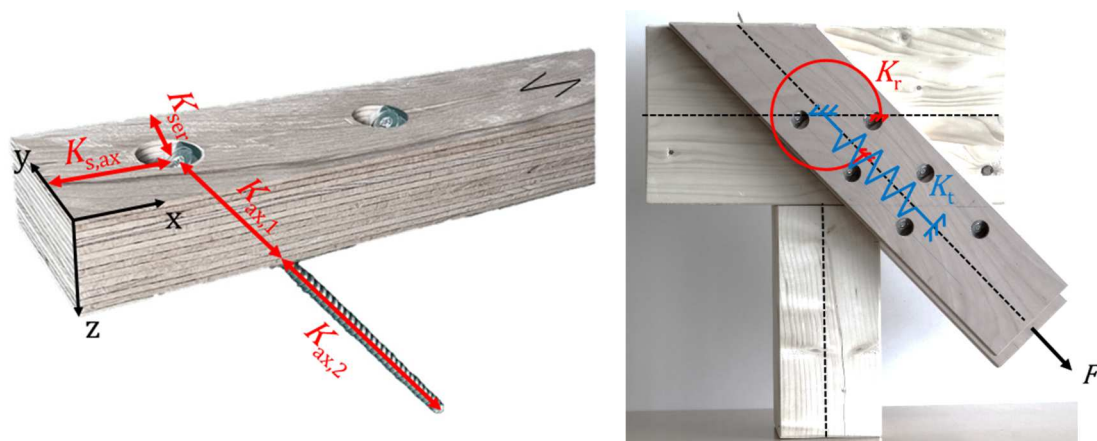


Fig. 3 – Differentiation of stiffness (left) and connection model with axially loaded screws (right).

$$K_{ser} = \rho_m^{1,5} * \frac{d}{23} \quad (2)$$

$$K_{ax} = 0,48 * d^{0,4} * l_{ef}^{0,4} * \rho^{0,3} \quad (3)$$

$$K_{s,ax} = \left(\frac{1}{\frac{1}{K_{ax,1}} + \frac{1}{K_{ax,2}}} \right) * \cos^2(\varepsilon) \quad (4)$$

Due to the different compliance in lateral and axial direction, K_{ser} according to equation (2) is significantly lower than K_{ax} according to (3), see for instance [3]. This difference is considered in equation (5) where K_{ser} becomes effective with increasing distances x and $K_{s,ax}$ with those for y , cf. Figure 5, right.

$$K_r = K_{ser} * \sum_{i=1}^n x_i^2 + K_{s,ax} * \sum_{i=1}^n y_i^2 \quad (5)$$

EXPERIMENTAL INVESTIGATIONS

Test set-up

The newly developed experimental set-up is shown in Figure 4. The core part of test apparatus consists of two mutually rotatable steel shells with rolling bearings between. Turning the inner shell against the outer one by pushing down the lever and simultaneous pulling at the side members enables the measurement of translational and rotational stiffness. Tension and rotation can be steered independently of each other so that rotational stiffness can be tested and quantified for different levels of tension. Deformations are tracked by digital image correlation.

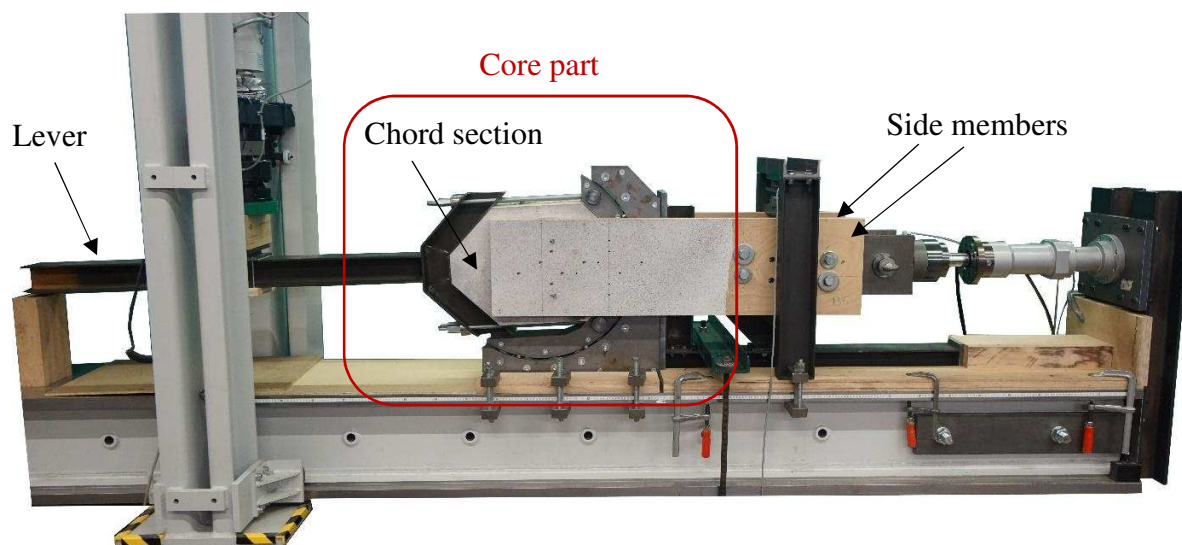


Fig. 4 – Test set-up with built-in specimen; side members stressed in tension; rotation by pushing down the left lever attached to the chord section.

Material and methods

The tests are carried out on test specimens with two side members made of 40 mm thick Be-LVL and an octagonal middle part made of softwood glulam. The connections are made with two or four fully threaded screws (8,0 x 240 mm) on each side. In addition to the number of screws, their position (Figure 5, left) and thus the polar moment of inertia of the connection are varied around the geometrical centre of gravity. This centre coincides with the actual pivot point of the inner shell. Figure 5, right illustrates how the screw stiffnesses K_{ser} and $K_{s,ax}$ and the respective distances x and y contribute to the rotational stiffness. In a first step, a tensile force in the range of a service load is applied to the connection. A rotation and the respective bending moment M is applied in a second step while the tensile force remains constant.

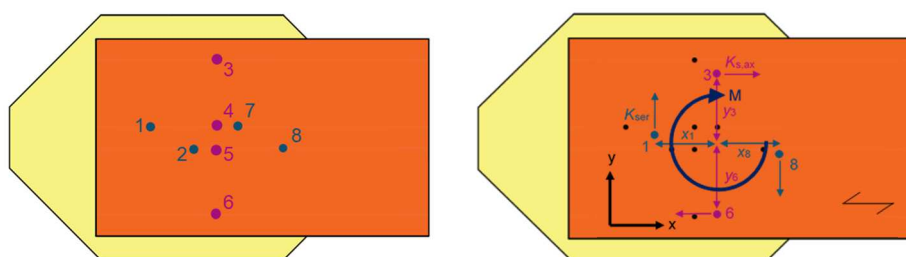


Fig. 5 – Screw position numbers (left) and mechanical definitions for the rotational stiffness (right).

Experimental test programme

The test programme shown in Table 1 encompasses 27 tests with 6 different screw arrangements. The screws are mainly loaded laterally or axially. The axial rigidity ($K_{s,ax} = 11.4$ kN/mm) is approximately 2.2 times higher than the lateral one ($K_{ser} = 5.14$ kN/mm). That effects 1.8 to 2.2 times higher rotational rigidities in series 4, 5 and 6 compared to the respective rigidities in series 1, 2 and 3. The small differences between single screw rigidities and rotational ones are due to the geometric specifications of the test specimens.

Table 1 – Experimental test programme.

Series	Number of tests	Number of screws	Position of screws	Traction	Squared distances to centre	Load direction
	[-]	[-]		[kN]	[mm ²]	
1	5	4	1+8	35	47900	Lateral
2	5	4	2+7	35	6480	Lateral
3	4	8	1+2+7+8	70	54400	Lateral
4	4	4	3+6	35	47900	Axial
5	4	4	4+5	35	6480	Axial
6	5	8	3+4+5+6	70	54400	Axial

Experimental results

Due to the rotation applied in the second step and the respective bending moment, the screws (Pos. No. 3 and 6) were subjected to an additional axial load. Screws (e.g. Pos. No. 3) where tension in the side members and simultaneous rotation cause axial stress in the same direction showed typical withdrawal failure in the Be-LVL side members and the shear plane remains closed. However, screws (e.g. Pos. No. 6) where tension and rotation causes opposed axial stresses behaved like compression struts. As a consequence, the shear plane between the chord section and the side members opened. Both effects are shown in the photographs in Figure 6.

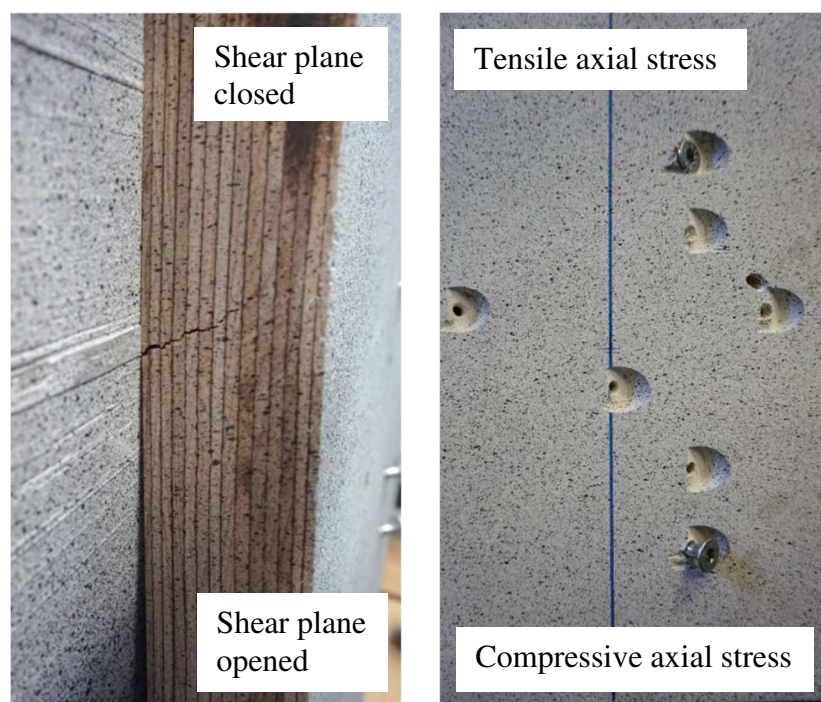


Fig. 6 – Deformed Be-LVL (left) due to relative screw movements in opposed directions (right).

The screws (Pos. No. 1 and 8) which receive an additional lateral load due to rotation were subjected to shear stress and thus formed two plastic hinges. The transversal pressure between the components caused tight contact. The relative rotational displacement in the shear plane becomes clear through the circular shaped abrasion of the paint, which mirrors on surface of the adjacent side member. This effect is illustrated in Figure 7.

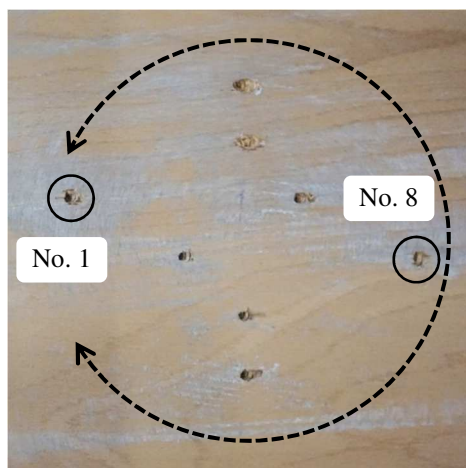


Fig. 7 – Circular shaped paint abrasion (highlighted by arrow) due to friction between the components.

The curves which represent the examined moment-rotation relationship are shown in the diagrams in Figures 8 to 10. In each diagram, the bending moment, calculated around the centre of gravity of the screw group, is plotted against the rotation. The curves of all tests prove that the test set-up and the test procedure enable reproducible test results. They feature only low scattering in their slope. Even the maximum moments of the respective series lie within a tight range. Between 0° and 0.3° (case by case up to 0.5°) the course of the curves is almost linear. In series one to three with mainly lateral stress of the screws, the initial linear course smoothly transitions into a second linear less inclined one. The rotation can be increased up to 3° (case by case up to 5°). After that, the moment resistance of the connection is reached. However, in series four to six with mainly axially loaded screws the curves transition into a non-linear course with horizontal tangent when the moment resistance becomes maximum. The respective plateaus end in the range between 2° and 4° with an abrupt drop of the moment.

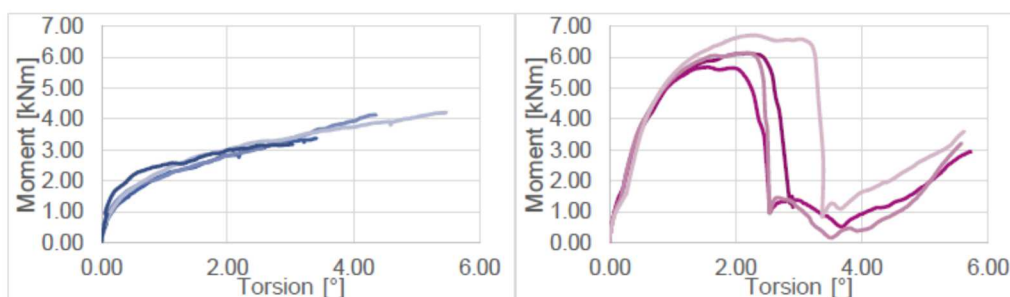


Fig. 8 – Torsional moment over rotational angle – Series 1 (left) and Series 4 (right).

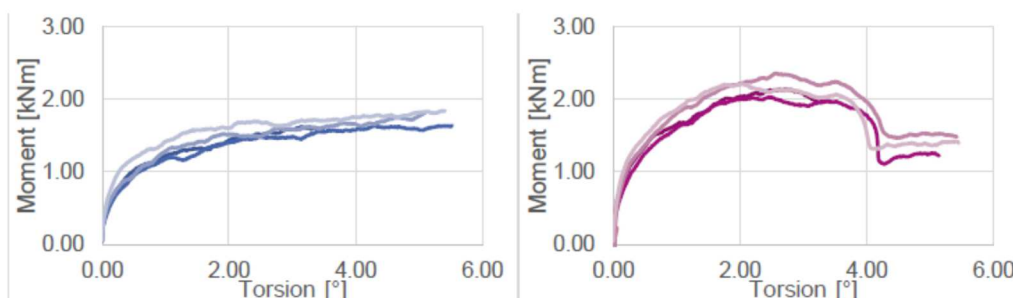


Fig. 9 – Torsional moment over rotational angle – Series 2 (left) and Series 5 (right).

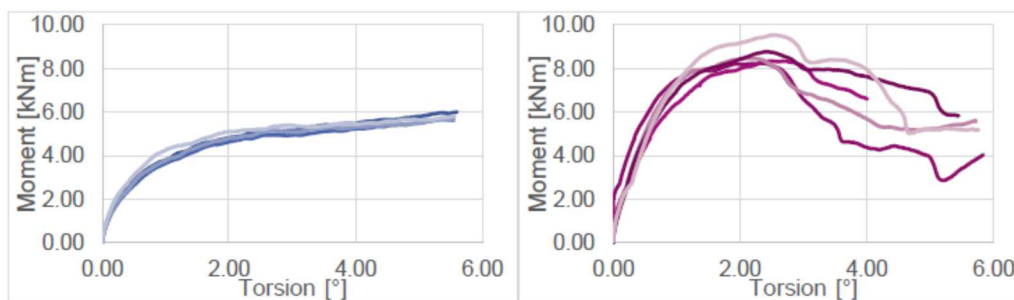


Fig. 10 – Torsional moment over rotational angle – Series 3 (left) and Series 6 (right).

Table 2 shows the maximum moments M_{max} , the rotational stiffness $K_{r,s}$ (between 10 % and 40 % of the maximum load) and $K_{r,i}$ (0 % to 40 % of the maximum load). The mean values and the coefficients of variation are shown for each series. The stiffnesses are determined according to DIN EN 26891:1991.

Table 2 – Mean values and COV of maximal torsional moment and modulus of rotation.

Series	M_{max}	ν	$K_{r,s}$	ν	$K_{r,i}$	ν
	[kNm]	[%]	[kNm/rad]	[%]	[kNm/rad]	[%]
1	3,92	11,8	188	3,51	238	3,34
2	1,73	6,58	189	28,1	249	27,8
3	5,80	2,76	332	15,4	406	16,5
4	6,17	6,87	402	10,9	479	11,0
5	2,18	6,27	264	23,8	326	24,6
6	8,68	6,00	585	34,7	742	38,4

COMPARISON BETWEEN ANALYTICAL AND EXPERIMENTAL RESULTS

Figure 11 shows a comparison between the analytical values K_r calculated according to equation (5) and the experimentally determined rotational stiffnesses $K_{r,s}$ and $K_{r,i}$. Equation (5) significantly underestimates the stiffness of connections with a small distance between the screws and their common centre of gravity. However, in the case of wider extended screw patterns with larger distances between screws and their centre of gravity equation (5) describes the stiffnesses relatively well. In 3 of 9 tests with wider extended patterns the stiffness $K_{r,i}$ is slightly overestimated. The reasons for the two symbols with high experimental values are not yet finally clarified.

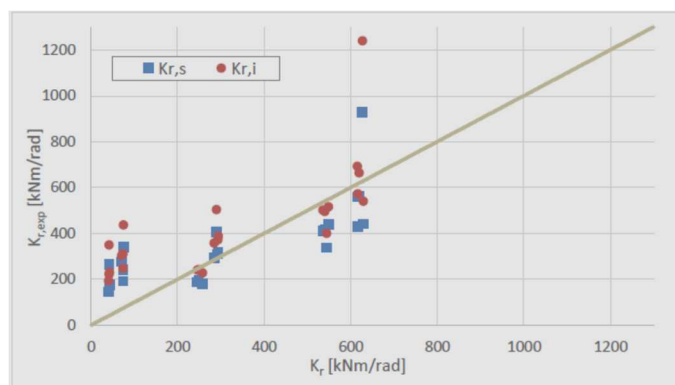


Fig. 11 – Comparison between analytical and experimental results.

In general, the results indicate that equation (5) has to be enhanced by a term for additional stiffness. This stiffness proportion is obviously caused by friction as a consequence of transversal pressure between the attached members. However, it is also conceivable that in the analytical model the proportion of screw stiffness might be overestimated by equation (2) or (3). It is not yet clear which of the different existing models for the axial stiffness is the most suitable for this examined mechanical issue.

CONCLUSIONS

The developed test set-up enables reproducible test results. The mechanical behaviour of the connections is as expected. They exhibit a linear relationship between moment and rotation for relative rotations up to 1°. Screw arrangements that experience additional axial load under subsequent rotation are stiff and feature high load-carrying capacities, but they are less robust and fail suddenly. Arrangements that experience lateral additional stress under subsequent rotation are less stiff and behave more ductile. Even under great rotation, they still remain viable. Comparisons between analytical and experimental results indicate that friction effects and the modelling of the axial screw stiffness are the main factors for the rotational stiffness. However, their respective share of the total rotational stiffness is not yet clarified. Further experiments are, therefore, required to better understand and more precisely quantify the influence of friction coefficients, fastener stiffness and preload.

ACKNOWLEDGMENTS

The authors gratefully acknowledge the financial support of the Federal Ministry of Food and Agriculture (BMEL) via the Agency of Renewable Resources (FNR) as project executing organisation (Code 22010017).

REFERENCES

- [1] Seige Y, Frese M, Study on a newly developed diagonal connection for hybrid timber trusses made of spruce glulam and beech laminated veneer lumber. In: *Wood Material Science and Engineering 14* (2019), pp.280-290.
- [2] Noguchi M, Komatsu K, A new method for estimating stiffness and strength in bolted timber-to-timber joints and its verification by experiments (II): bolted cross-lapped beam to column joints. In: *The Japan Wood Research Society 50* (2004), pp.391-399.
- [3] Schweigler M, Bader T, Hochreiner G, Unger G, Eberhardsteiner J, Load-to-grain angle dependence of the embedment behavior of dowel-type fasteners in laminated veneer lumber. In: *Construction and Building Materials 126* (2016), pp.1020-1033.
- [4] Ringhofer A, Burtscher M, Sieder R, Gstetter M, Self-tapping Timber Screws Subjected to Combined Axial and Lateral Loading. In: *INTER 54* (2021), pp.95-111.
- [5] De Santis Y, Fragiaco M, Slip modulus formulas for timber-to-timber inclined screw connections – Comparison with other simplified models. In: *INTER 54* (2021), pp.131-145.
- [6] Blass HJ, Steige Y, Steifigkeit axial beanspruchter Vollgewindeschrauben. *Karlsruher Berichte zum Ingenieurholzbau, Band 34*, KIT Scientific Publishing, 2018.